# Feature Extraction Evaluation for Two Motor Imagery Recognition Based on Common Spatial Patterns, Time-Frequency Transformations and SVM

Mario I. Chacon-Murguia
*Visual Perception Laboratory*
*Tecnologico Nacional de Mexico /*
*Instituto Tecnologico de Chihuahua*
Chihuahua, Chih., Mexico
mchacon@ieee.org

Eduardo Rivas-Posada
*Visual Perception Laboratory*
*Tecnologico Nacional de Mexico /*
*Instituto Tecnologico de Chihuahua*
Chihuahua, Chih., Mexico
eduardo.rivasp@ieee.org

***Abstract*— In recent years, motor imagery has been used as a communication alternative in brain computer interface systems. In this paper an evaluation of five different types of feature extraction methods to recognize two motor imagery signals based on common spatial patterns (CSP), and time-frequency transformations are evaluated; CSP, continuous Wavelet transform (CWT), Stockwell transform (ST), and the following combinations CSP+CWT and CSP+ST. The classifier employed to recognize between right-hand, and left-hand was a support vector machine. The proposed methods were evaluated in two know datasets and compared with other state of the art methods. The best performance achieved with the proposed methods, considering a correct recognition rate, was 79.87% ± 10.73% and 73.25% ± 08.04% with the datasets BCI Competition IV dataset 2a and *EEGdataset*, showing better performances than the reported works. Besides, the CSP+SVM method requires a processing time of only 1.73 seconds which make it suitable for real time applications.**

***Keywords—Motor imagery, real time BCI, SVM, CSP, CWT.***

## I. INTRODUCTION

In recent years, research in brain computer interfaces, BCI, has highly increased. One of the more complex and challenged BCI systems are the one based on motor imagery, MI. An MI can be considered as a mental execution of a motor act without a physical performance [1]. The brain activity of a MI is captured by electrodes commonly using an electroencephalogram, EEG. This signal involves sensorimotor rhythms, as well as μ (7.5-12Hz) and β (12-30Hz) waves. The MI approach is preferred to other BCI approaches because, it does not require external stimulus to generate the BCI signals. That is, the BCI system does not need external devices or circuitry to produce the EEG signals.

In a previous work [2] , the authors presented a methodology to classify MI related to feet and the right hand using statistical moments. The performance achieved was close to 90%. However, the proposed method cannot be implemented in real time. It just works off-line.

According to [3] a MI presents an event-related desynchronization or ERD with a duration between 1500ms and 2000ms. Therefore, to consider that a BCI system works in real time, the entire classification process, from data acquisition, processing, and MI assignation, needs to be less than 3 seconds. This is because in 3 seconds 2 ERD events can occur, data information from a MI is lost and the system is no longer considered in real time.

Therefore, considering this restriction and the results of other works reported in the literature [4], [5], [6], [7], [8], it was considered to do a more complete analysis and evaluation of BCI methods to be able to design a new one that can be implemented for real time applications. This work describes the evaluation of 5 methods base on common spatial patterns (CSP), and time-frequency transformations. The CSP methods analyzed were the works reported in [9], [6], [10], [11]. The methods based on time-frequency, like Wavelet or Stockwell are reported in [4] and [12], respectively.

The second contribution of this work is that as our knowledge, the CSP and the time-frequency approaches have been reported as separated methods, and they have not been reported as a fused method used in real time applications. The combination of spatial patterns and transformations in time-frequency allows to extract features that, according to some evidence, can help to detect MI even from subjects whose MI are not so evident. Thus, this work proposes a new approach to classify MI signals by fusing CSP and time-frequency methodologies which can be used in real time applications.

The paper is organized as follows. General information of the EEG signal processing is described in section II. Section III presents the feature extraction stage. The classification stage is reported in Section IV, and the results and conclusions are presented in section V and VI, respectively.

## II. EEG SIGNAL PROCESSING

The general scheme of the proposed methodology to recognize MI is illustrated in Fig. 1. This scheme involves six main stages: EEG signal extraction, signal preprocessing, epoch extraction, data augmentation, feature extraction, and classification. The explanation of each one of these stages is provided in the next sections.

### *A. EEG signal extraction*

The EEG signals are obtained from the following databases.

*1) BCI Competition IV dataset 2a*

The database *BCI Competition IV dataset 2a* [13] was selected because it is broadly used in other works reported in the

978-1-7281-6926-2/20/$31.00 ©2020 IEEE

literature, and it provides a good mean of performance comparison. This dataset includes the next characteristics:

- 4 MI (left-hand, right-hand, both feet, and tongue motion).
- 9 subjects perform a training session and a test session.
- 288 essays for session, 72 essays for class.
- The EEG signals were registered with 22 Ag/AgCl electrodes, therefore the number of channels $nCh = 22$.
- The sampling frequency Fs = 250 Hz. A 0.5 Hz to 100 Hz band pass filter was applied.

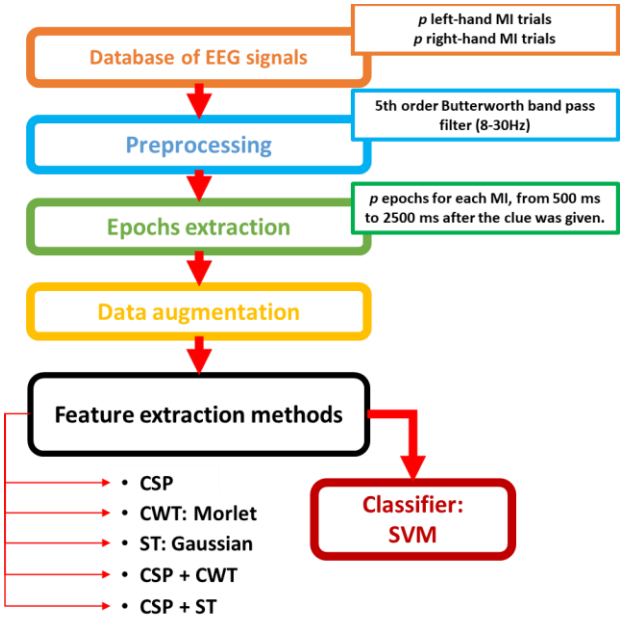


Fig. 1. General scheme of the proposed methodology to recognize MI.

*2) EEGdataset*

The dataset *EEGdataset* was obtained from [14]. It was selected because it includes many subjects. It is one of the most up to date datasets (2017) and presents the following characteristics:

- 2 MI (left-hand, and right-hand).
- 52 subjects.
- One session with 100 to 120 essays for each class.
- The EEG signals were registered with 64 Ag/AgCl electrodes, therefore $nCh = 64$.
- The sampling frequency Fs = 512 Hz.
- Raw data.

## B. Preprocessing

Let $Xraw^{Ch}(n) \in \mathbb{R}^{nCh \times N}$ be the discrete signal which contains $N$ raw data of and EEG channel $Ch$, obtained with a sampling frequency $Fs$, from each subject and from each one of the datasets. In the case of the *BCI Competition IV dataset 2a* only the left, and right-hand MI signals were considered.

The signal $Xraw^{Ch}(n)$ was filtered with a fifth order band-pass IIR Butterworth digital filter, with cut frequencies corresponding to the frequencies of the waves *mu* and *beta*, 7.5Hz to 30Hz. This filter allows a monotonic response in the band pass up to the cut frequency, and the magnitude of the raw data is not modified. The difference equation of the filter is

$$Xfilt^{Ch}(n) = \sum_{i=0}^{5} b_i Xraw^{Ch}(n-i) - \sum_{i=1}^{5} a_i Xfilt^{Ch}(n-i) \quad (1)$$

where $a$ and $b$ are the coefficients of the filter and $Xfilt^{Ch}(n) \in \mathbb{R}^{nCh \times N}$ is the input EEG signal of each Chanel $Ch$ for subject for dataset.

## C. Epochs extraction

This stage consists on extraction $p$ epochs for each MI class of each session to reduce the data dimensionality, and to extract the relevant information of the filtered signal. An epoch is defined as

$$\begin{gathered} x_{ep}^{Ch}(k) = Xfilt^{Ch}(q_{ep} + k + inc) \\ ep = 1,2,\ldots,p \\ k = 1,2,\ldots,2Fs \\ x_{ep}^{Ch}(k) \in \mathbb{R}^{nCh \times 2Fs \times p} \end{gathered} \quad (2)$$

where $k$ is the data index in the epoch $x_{ep}^{Ch}$ of the channel $Ch$ and $q_{ep}$ refers to the initial sample of the MI in the epoch $ep$. Therefore, there are $p$ epochs of two seconds ($2Fs$ samples) of each channel $Ch$ of each MI.

At the first instance $inc$=45 (number of samples that correspond to 80ms at $Fs$=250Hz), because it is intended to obtain an epoch going from 180ms after the beginning of the MI ($q_{ep} + inc$) to 2180ms ($q_{ep} + 2Fs + inc$). This interval is selected due to the fact that an MI presents a ERD with a duration of 1500ms to 2000ms [3], and thus assuring to obtain an adequate information to analyze the type of MI.

## D. Data augmentation

In order to represent better each MI class, it is necessary to increment the number of samples in the EEG signal under analysis[15]. Data augmentation is achieved by overlapping windows of 80ms in 80ms that involve the MI event under screening. In this way the most important information with only a few modifications is preserved [16]. Therefore, $inc$ takes different values in (2)

$$inc = 45 + (20)(l) \quad l = 0,1,2,\ldots,9 \quad (3)$$

$inc$ takes 10 different values from 45 (180ms) to 225 (900ms), by the increments of 20 samples every 80ms. This results in the generation of 10 epochs per essay instead one epoch per essay. The first epoch will cover the interval in the MI event form 180ms to 2210ms and the last one from 900ms to 2900ms. These data were divided into two sets: 8$p$ epochs of MI that represent 80% of the simples were employed for training, and the other 20% for validation.

# III. Feature Extraction

This section presents the five methods used for feature extraction that were tested in this work: CSP, continuous Wavelet transform (CWT), Stockwell transform (ST), and the following combinations CSP+CWT and CSP+ST. In the next

paragraphs each feature extraction method is explained and the classifier to recognize right and left-hand MI recognition using the previous features will be analyzed.

### A. Method 1: CSP

By using CSP we try to do a linear transformation which projects a multichannel EEG signal into a subspace of lower dimension. This process allows to use information from both classes and eliminate redundant information. The CSP are generated by considering two MI classes: right and left-hand, denoted as

$$C = \{c_{izq}, c_{der}\} \tag{4}$$

The normalized covariance matrix of each class is obtained by

$$\overline{Cov}_C = \sum_{ep=1}^{8p} \frac{\left[x_{ep}\right]\left[x_{ep}\right]^T}{trace\left\{\left[x_{ep}\right]\left[x_{ep}\right]^T\right\}} \qquad \overline{Cov}_C \in \mathbb{R}^{nCh \times nCh} \tag{5}$$

where *trace*() indicates the trace of the input matrix, considering $8p$ epochs of each MI to obtain the normalized covariance of each class in the training stage.

Then, the spatial covariance, which allows the best discrimination of classes is computed

$$Cov = \overline{Cov}_{der} + \overline{Cov}_{izq} = UDU^T \tag{6}$$

here $U$ is the eigenvector array of $Cov$ and $D$ is the diagonal matrix with the eigenvalues of $Cov$, sorted in descending order. The next step is to obtain the whitening transformation matrix

$$P = D^{-1/2}U^T \tag{7}$$

This process allows to normalize $D$ to one, generating a space where the data variances that will be filtered with the spatial filter assume values in [0,1]. Besides, if $\overline{Cov}_{der}$ and $\overline{Cov}_{izq}$ are transformed as

$$G_{der} = P\overline{Cov}_{der}P^T \qquad G_{izq} = P\overline{Cov}_{izq}P^T \tag{8}$$

then $G_{der}$ and $G_{izq}$ will share common eigenvectors through the eigenvalues $\lambda_1$ and $\lambda_2$

$$G_{der} = U_G \lambda_1 U_G{}^T \qquad G_{izq} = U_G \lambda_2 U_G{}^T \tag{9}$$

and their sum is the identity matrix

$$\lambda_1 + \lambda_2 = I \tag{10}$$

As a result, the eigenvectors with the largest eigenvalues for $G_{der}$ correspond to the smallest eigenvalues for $G_{izq}$, and vice versa. Such that the spatial filter matrix is defined by

$$W_{CSP} = U_G^T P \quad ; \quad W_{CSP} \in \mathbb{R}^{nCh \times nCh} \tag{11}$$

In the resulting spatial filters, the rows correspond to the combined information of both classes of each channel employed to obtain the EEG signal. This information is arranged in descending order where the first row has the highest variance.

The transformation of each epoch is by using the first row and the row $nCh$ of the spatial filter

$$\mathbf{Z}_{CSP}^{fil}(k) = \left[W_{CSP}^{fil}\right]^T \left[x_{ep}(k)\right]; \quad \mathbf{Z}_{CSP}^{fil}(k) \in \mathbb{R}^{2\times 2Fs\times 8p} \tag{12}$$

where *fil* represents each row used in the transformation. This produces a reduction of the data dimension and concatenate the two rows with higher variances to obtain the matrices $\mathbf{Z}_{CSP}^{fil}(k)$.

After the previous step, the logarithm of the variances is computed in order to reduce the variation among large values, and thus obtain a gaussian distribution [17], of each row *fil* of $\mathbf{Z}_{CSP}^{fil}(k)$ for each one of the epochs

$$y_{CSP}^1 = \log\left\{\text{var}\left[Z_{CSP}^1\right]\right\}\Big|_1^{8p} \qquad y_{CSP}^2 = \log\left\{\text{var}\left[Z_{CSP}^2\right]\right\}\Big|_1^{8p} \tag{13}$$

here $y_{CSP}^1$ and $y_{CSP}^2$ correspond to the two extracted features for each one of the $8p$ MI. That is, $\Gamma_{CSP}^{fil} = (y_{CSP}^1, y_{CSP}^2)$, $\Gamma_{CSP}^{fil} \in \mathbb{R}^{2\times 8p}$ are the feature vectors for the support vector machine (SVM) classifier.

### B. Method 2: CWT

This method involves the continuous Wavelet transform, using the Morlet wavelet. The CWT was applied on the channels C3 and C4 of each one of the $8p$ epochs

$$\mathbf{Z}_{CWT}^{Ch,Sc}(k) = abs\left(\text{CWT}\left\{x_{ep}^{Ch}(k)\right\}\right) \qquad Ch = \{C3, C4\} \tag{14}$$

where $\mathbf{Z}_{CWT}^{Ch,Sc}(k) \in \mathbb{R}^{Sc\times 2Fs\times 8p}$. The coefficients used of the transform were obtained by sampling the CWT. Both the minimum and maximum scales of the CWT are determined automatically as a function of the energy distribution the CWT represented in a logarithmic scale [18]. Therefore, $Sc$ is the number of frequency scales obtained from the transformation, where the band of 7.5Hz to 28Hz was selected because it includes the sensory motor rhythms.

Next, it is proposed to use the average of the natural logarithms of the sum of the absolute values of $\mathbf{Z}_{CWT}^{Ch,Es}(k)$ of each channel to compare the energy of the CWT of the channels C3 and C4

$$y_{CWT}^{C3} = \frac{1}{Sc}\ln\sum_{Es}\left|Z_{CWT}^{C3,Sc}\right|\Big|_1^{8p} \qquad y_{CWT}^{C4} = \frac{1}{Sc}\ln\sum_{Es}\left|Z_{CWT}^{C4,Sc}\right|\Big|_1^{8p} \tag{15}$$

here $y_{CWT}^{C3}$ and $y_{CWT}^{C4}$ represent the two characteristics obtained from each MI. That is $\Gamma_{CWT}^{Ch} = (y_{CWT}^{C3}, y_{CWT}^{C4})$, $\Gamma_{CWT}^{Ch} \in \mathbb{R}^{2\times 8p}$ are the input feature vectors for the SVM classifier. In this method and in the other methods, it was decided to use ln, instead log, because ln yields a higher discrimination between the data, and therefore a better recognition performance.

### C. Method 3: ST

This third method uses the Stockwell transform, over the channels C3 and C4 of each one of the epochs, employing variable gaussian windows

$$\mathbf{Z}_{ST}^{Ch,F}(k) = abs\left(\text{ST}\left\{x_{ep}^{Ch}(k)\right\}\right) \tag{16}$$

where $\mathbf{Z}_{ST}^{Ch,F}(k) \in \mathbb{R}^{F\times 2Fs\times 8p}$ and $F$ are frequencies (from 1 to Fs Hz) obtained from the transformation, represented with a resolution of 1Hz, selecting the band 8Hz to 28Hz, because it contains the sensory motor signals. Unlike the CWT, in the ST transform the range of frequencies of 8Hz to 28Hz was used instead the band 7.5Hz to 28Hz, because the ST has a resolution of 1Hz, and the resolution of the CWT is a function of the resulting scales of the transform.

Next, the average of the natural logarithms was computed over the sum of absolute values of $\mathbf{Z}_{ST}^{Ch,F}(k)$, for each channel

$$y_{ST}^{C3} = \frac{1}{F}\ln\sum_{F}\left|Z_{CWT}^{C3,F}\right|_{1}^{8p}$$
$$y_{ST}^{C4} = \frac{1}{F}\ln\sum_{F}\left|Z_{CWT}^{C4,F}\right|_{1}^{8p} \quad (17)$$

here $y_{ST}^{C3}$ and $y_{ST}^{C4}$ correspond to the two features extracted from each MI, that is, $\Gamma_{ST}^{Ch} = (y_{ST}^{C3}, y_{ST}^{C4})$, $\Gamma_{ST}^{Ch} \in \mathbb{R}^{2\times 8p}$ which are the input feature vectors for the SVM.

### D. Method 4: CSP+CWT

This method involves the combination of the features extracted with the CSP, and the CWT. The CSP was used to automatically select the two rows of the filter $W_{CSP}$ that include information with the highest variance of both classes. CWT was used to process this information. Therefore, the CWT was obtained from the matrix yielded by the CSP

$$\mathbf{Z}_{CSP\_CWT}^{fil,Sc}(k) = abs\left(\mathrm{CWT}\left\{\mathbf{Z}_{CSP}^{fil}(k)\right\}\right) \quad (18)$$

where $\mathbf{Z}_{CSP\_CWT}^{fil,Sc}(k) \in \mathbb{R}^{Sc\times 2Fs\times 8p}$ is the absolute value obtained from the selection of the combined information of both classes of the two selected channels by the CSP.

According to [19], and [20] a MI of the right-hand, will present more energy in the contralateral zone of the brain, left channels in this case, and a MI of the left-hand in the right channels. Assuming this information, the figures shown in Fig. 2 can be analyzed as follows.

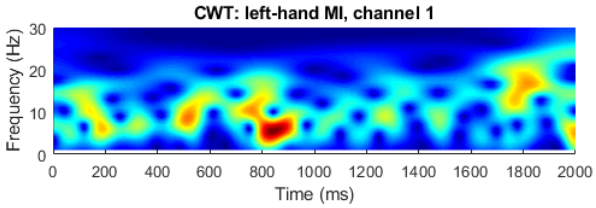


a) CWT of the MI of the left-hand using channel 1.

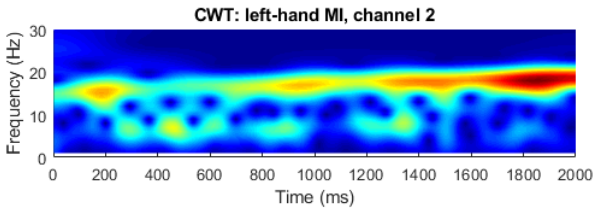


b) CWT of the MI of the left-hand using channel 2.

Fig. 2. Example of the CWT of the MI of the left hand.

Fig. 2 illustrates the CWT of the dataset *EEGdataset* of subject 14. The channels shown correspond to the channels selected with the CSP filters. Channel 1 correspond to the left side and channel 2 to the right. The graph axes correspond to the frequencies of the sensory motor frequencies in two second of samples. It can be observed the distribution of energy present in the CWT of the MI of the left hand. This distribution shows a higher uniform energy in the second channel, which is expected for this MI.

The case of the MI of the right-hand is presented in Fig. 3. In this case as commented before the energy distribution is contrary to the left hand, and it appears in channel 1.

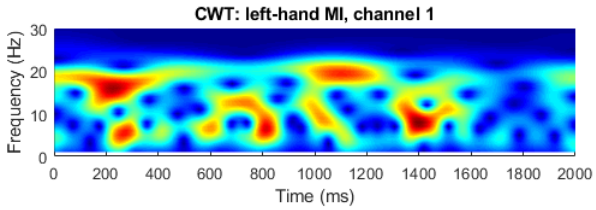


a) CWT of the MI of the right-hand using channel 1.

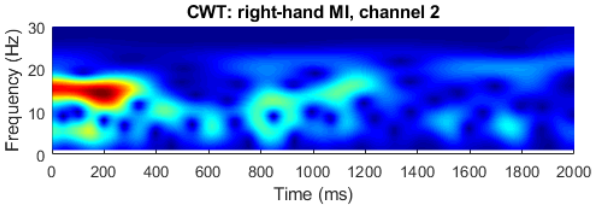


b) CWT of the MI of the right-hand using channel 2.

Fig. 3. Example of the CWT of the MI of the right-hand.

### E. Method 5: CSP+ST

This method is like method 4, but instead using the CWT, it was employed the ST. The CSP filters select the best channels, and the ST is used to analyze and select the time-frequency features

$$\mathbf{Z}_{CSP\_ST}^{fil,F}(k) = abs\left(\mathrm{ST}\left\{\mathbf{Z}_{CSP}^{fil}(k)\right\}\right) \quad (19)$$

here $\mathbf{Z}_{CSP\_ST}^{fil,F}(k) \in \mathbb{R}^{F\times 2Fs\times 8p}$ is the absolute value obtained from the selection of the combined information of both classes of the two selected channels by the CSP.

## IV. Classifier

The SVM allows to find a discriminant hyperplane between classes by maximizing the margins between the classes. The hyperplane may be represented by

$$\mathcal{G}(\Gamma) = W_{SVM}^{T}\Gamma + W_{0\_SVM} \quad (20)$$

where $W_{SVM}$ is the weight vector, $\Gamma$ are the input data, and $W_{0\_SVM}$ is a scalar to adjust the hyperplane *off-set*. The SVM methodology intents to optimize the margin between the two classes. The samples that correspond to this optimization are termed support vectors. The optimization problem can be stated as

$$\min \mathcal{L}\left(W_{SVM},\xi\right)=\frac{1}{2}\left\|W_{SVM}\right\|^2+\sum_{i=1}^{n}\iota_i\xi_i \qquad (21)$$
$$w\in W_{SVM},\quad \iota\geq 0$$

Such that $\Upsilon_i\left[W_{SVM}^T\Gamma_i+W_{0\_SVM}\right]\geq 1-\xi_i$ for $\xi_i\geq 0$ and $i=(1,\ldots,n)$. Where $\Upsilon\in\{+1,-1\}$ denotes the class label, $\xi$ is a *slack* factor that allows to the inequality restriction to be transformed into an equality, and $\iota$ are the Lagrange factors. A radial base *kernel* was used in all the methodologies

$$\Phi\left(y_\delta,y_\upsilon\right)=\exp\left(-\left\|y_\delta-y_\upsilon\right\|^2\right) \qquad (22)$$
$$y_\delta,y_\upsilon\in\Gamma$$

$y_\delta, y_\upsilon$ are n-dimensional vectors that represent the observations $\delta$ and $\upsilon$ in $\Gamma$, modifying (20) into

$$\mathcal{G}\left(\Phi\right)=W_{SVM}^T\Phi+W_{0\_SVM} \qquad (23)$$

Therefore, by substituting (22) into (23) we obtain the SVM classification function with the *kernel* with radial base radial

$$\mathcal{G}\left(\Gamma\right)=W_{SVM}^T\exp\left(-\left\|y_\delta-y_\upsilon\right\|^2\right)+W_{0\_SVM} \qquad (24)$$

It can be observed from (24) that only two features are used. This model was selected and tested because we intended to use a simple computational classifier, in order to achieve to try to design a real time BCI.

## V. Results

The performances of the proposed methods using the SVM as the classifier were obtained by using the provided *Ground Truth* in the datasets, and the metric of correct classification considering the average performance over all the experiments.

Table I shows the performances for training and validation using the different methods to extract features of the MI signals. $CSP_2$ indicates the use of two rows of the projection matrix, and SVM is the classifier. The dataset evaluated is *BCI Competition IV dataset 2a.* Table II presents the results for the dataset *EEGdataset*.

TABLE I. Performance for the dataset BCI Competition IV dataset 2a.

| **Method** \Evaluation | Training | Validation | Average |
|---|---|---|---|
| **$CSP_2$+SVM** | **80.16% ± 10.56%** | **79.57% ± 10.89%** | **79.87% ± 10.73%** |
| CWT+SVM | 64.39% ± 07.46% | 64.43% ± 07.32% | 64.41% ± 07.39% |
| ST+SVM | 64.46% ± 07.91% | 62.50% ± 07.75% | 63.48% ± 07.83% |
| $CSP_2$+CWT+SVM | 79.82% ± 11.27% | 77.93% ± 12.88% | 78.87% ± 12.08% |
| $CSP_2$+ST+SVM | 78.07% ± 11.36% | 76.93% ± 13.08% | 77.50% ± 12.22% |

These results can be compared directly with the average performance of 67.46% ±13.17% of the work reported in [14] that employs CSP for feature extraction, and a Fisher linear discriminant classifier. Besides, the authors in [14] mentioned in their work that the subjects 29 and 34 were discarded because their signal were correlated with electromyographic signals in most of their 90% essays, producing higher energy in the frequency band of 50Hz to 250Hz. During their MI events.

TABLE II. Performance for the dataset *EEGdataset*

| **Method** \Evaluation | Training | Validation | Average |
|---|---|---|---|
| **$CSP_2$+SVM** | 73.66% ± 07.60% | **72.83% ± 08.48%** | **73.25% ± 08.04%** |
| CWT+SVM | 66.94% ± 05.31% | 65.56% ± 05.97% | 66.25% ± 05.64% |
| ST+SVM | 65.94% ± 05.76% | 64.42% ± 07.22% | 65.18% ± 06.49% |
| $CSP_2$+CWT+SVM | **73.87% ± 07.65%** | 72.49% ± 07.97% | 73.18% ± 07.81% |
| $CSP_2$+ST+SVM | 72.53% ± 07.37% | 70.89% ± 07.93% | 71.71% ± 07.65% |

Unlike the work presented in [14], we decided to include the subjects 29 and 34 because our analysis is based on CSP and time frequency features, which allows that even if there is a correlation with other type of signals, the brain activity is present, and our model will be able to determine the correct features to distinguish between the left and right-hand MIs.

Table III shows the training and validation results for the subject 29 of the dataset *EEGdataset* using our different proposed methods. The evaluation for the subject 34 is shown in Tab. IV.

TABLE III. Performance of the subject 29 of the dataset *EEGdataset* obtained with our proposed methods

| **Subject 29 of *EEGdataset*** | | | |
|---|---|---|---|
| **Method** \Evaluation | Training | Validation | Average |
| $CSP_2$+SVM | 63.25% | 63.00% | 63.13% |
| **CWT+SVM** | **64.81%** | **67.25%** | **66.03%** |
| ST+SVM | 64.19% | 59.25% | 61.72% |
| $CSP_2$+CWT+SVM | 61.06% | 64.75% | 62.91% |
| $CSP_2$+ST+SVM | 64.31% | 65.00% | 64.66% |

TABLE IV. Performance of the subject 34 of the dataset EEGdataset obtained with our proposed methods

| **Subject 34 of *EEGdataset*** | | | |
|---|---|---|---|
| **Method \Evaluation** | Training | Validation | Average |
| $CSP_2$+SVM | **65.81%** | 63.00% | 64.41% |
| CWT+SVM | 65.69% | 60.25% | 62.97% |
| ST+SVM | 59.25% | 58.00% | 58.63% |
| $CSP_2$+CWT+SVM | 63.88% | 62.50% | 63.19% |
| **$CSP_2$+ST+SVM** | 65.63% | **67.25%** | **66.44%** |

From the previous tables, it can be noticed that the average performance of the subject 29 was 66.03% using the method CWT+SVM and the performance of the subject 34 was 66.44% with $CSP_2$+ST+SVM. These results compared with the results reported in [14], indicate that our proposed methodology can be used in cases where other methods are not able to produce acceptable results.

A more complete comparison of our proposed methods against other works reported in the literature are shown in Table V. The table provides information regarding; feature extraction methods, type of classifier, number of MI to recognize, number of subjects evaluated, performances, and the year of the work.

TABLE V. PERFORMANCE COMPARISON OF THE PROPOSED METHODS WITH OTHER STATE OF THE ART METHODS

| Feature extraction | Classifier | No. of MIs | No. of subjects | Performance | Database | Approx. Processing time (sec) | Computer system | Ref. | Year |
|---|---|---|---|---|---|---|---|---|---|
| FFT - WPD | Deep learning based on RBM | 2 MIs | 9 | 84% ± 11.93% | BCI Competition IV dataset 2b | 3.43 | Dual core processor i7-3700 / 3.40GHz / 12 GB RAM | [21] | 2017 |
| CSP | Fisher linear discriminant | 2 MIs | 52 | 67.46 ± 13.17% | *EEGdataset* | 2 | - | [17] | 2017 |
| CSPO | TWSVM | 2 MIs | 9 | 75.93% | BCI Competition IV dataset 2a | 0.0256 | Windows 7 / Intel Core i3-4030U CPU (1.90 GHz) / 4 GB RAM | [10] | 2017 |
| CWT | CNN | 2 MIs | 9 | 78.93 ± 6.83% | BCI Competition IV dataset 2b | - | - | [4] | 2018 |
| PSD | CNN | 3 MIs | 8 | 62.1 ± 15% | Their own dataset | - | - | [5] | 2018 |
| CSP-LBP | LDA | 2 MIs | 8 | 76.46% | Their own dataset | 2 | Windows 8 / Intel i3 Core / 2.30GHz processor | [11] | 2019 |
| RCT | ANN | 2 MIs | 1 | 84.40% | BCI Competition II dataset III | 5.25 | - | [22] | 2019 |
| TSGSP | SVM | 2 MIs | 9 | 82.51% ± 12.24% | BCI Competition IV dataset 2a | 17 | 1.99 GHz CPU / i7-8550U / 16GB RAM | [23] | 2019 |
| JSTFD | LDA | 2 MIs | 9 | 79.6% ± 14.7% | BCI Competition IV dataset 2a | 17.11 | Intel® Xeon® CPU E5-2620 v4 @ 2.10GHz processor / 64GB RAM | [24] | 2020 |
| $CSP_2$ | SVM | 2 MIs | 9 | 79.87% ± 10.73% | BCI Competition IV dataset 2a | 1.73 | Windows 10 / Intel® Xeon® E5-1620 v3 3.50GHz /16 GB RAM | Our method | |
| $CSP_2$ | SVM | 2 MIs | 52 | 73.25% ± 08.04% | *EEGdataset* | 1.73 | | | |

The works of Table V were selected because they classify the same number of MIs (except [5]), use known databases and form part of the state of the art methods.

The work described in [21] indicates that for each data training set, the preprocessing time, including the FFT takes 1.39 seconds, feature extraction preparation takes 12.38 seconds, the training stage 98.84 seconds, and the testing stage 2.04 seconds. In the case of our proposed method $CSP_2$+SVM, which is the method with the best results, the times are indicated next. Preprocessing time 1.65 seconds, feature extraction preparation 1.1 seconds, training stage 0.86 seconds, and testing 0.08 seconds. Therefore, considering the processing time plus the testing time (without considering the preparation time) the time reported in [21] will be 3.43 seconds, which won't be able to process the MI in real time. On the other hand, in the method $CSP_2$+SVM will be able to process in real time because it takes only 1.73 seconds, approximately half the time of the method in [21].

Considering the same reasoning, only the works described in [17] and [11] could be considered as a real time methods because they complete processing time in 2 seconds. The works presented in [22], [23] and [24] report high performances, however they report too high times to be considered real time systems, specially [23] and [24]. The evaluation of the method reported in [22] was included in this Table V, because it presents the highest performance, however its processing time is high, and it was only tested with one subject. Unfortunately, the works reported in [4] and [5] did not provide they processing times.

## VI. CONCLUSIONS

This work reports a new methodology to recognize two types of MI, left and right-hand. The work proposed five different methods for feature extraction, based on common spatial patterns, and time frequency transforms: $CSP_2$, CWT, ST, $CSP_2$+CWT and $CSP_2$+ST. The highest performance achieved was 79.87% with the dataset *BCI Competition IV dataset 2a* and 73.25% with the dataset *EEGdataset* using $CSP_2$ in combination with the SVM classifier. The method performs the recognition in 1.73 seconds, making it a competitive method for real time BCI.

As the results have been favorable to implement this methodology in real time, a future work will be to generate a new database to includes more motor imageries to detect the visualizations of tongue and foot movement. Another future work is to implement a classifier based on deep neural networks aimed to improve the performance of MI recognition.

## ACKNOWLEDGMENT

This research was funded by Tecnologico Nacional de Mexico/ I.T. Chihuahua under grant 5684.16-P.

## REFERENCES

[1] G. Pfurtscheller and C. Neuper, "Motor imagery and direct brain-computer communication," *Proc. IEEE*, vol. 89, no. 7, pp. 1123–1134, 2001.

[2] E. Rivas-Posada, M. I. Chacon-Murguia, and J. A. Ramirez-Quintana, "Classification of motor imagery using statistical models," in *2019 16th International Conference on Electrical Engineering, Computing Science and Automatic Control, CCE 2019*, 2019, pp. 1–6.

[3] M. X. Cohen, *Analyzing Neural Time Series Data : Theory and Practice.*, MIT Press. Cambridge, MA: 1 edition, p. 600, 2014.

[4] H. K. Lee and Y.-S. Choi, "A Convolution Neural Networks Scheme for Classification of Motor Imagery EEG based on Wavelet Time-

Frequecy Image," in *2018 International Conference on Information Networking (ICOIN)*, 2018, pp. 2–5.

[5] L. G. Hernandez and J. M. Antelis, "A Comparison of Deep Neural Network Algorithms for Recognition of EEG Motor Imagery Signals," *Pattern Recognition*, vol. 10880, Springer, Cham, pp. 126–134, 2018.

[6] T. Nguyen, I. Hettiarachchi, A. Khatami, L. Gordon-Brown, C. P. Lim, and S. Nahavandi, "Classification of Multi-Class BCI Data by Common Spatial Pattern and Fuzzy System," *IEEE Access*, vol. 6, pp. 27873–27884, 2018.

[7] T. Uktveris and V. Jusas, "Convolutional neural networks for four-class motor imagery data classification," in *Intelligent Distributed Computing XI. IDC 2017.*, Springer,., vol. 737, S. M. (eds) Ivanović M., Bădică C., Dix J., Jovanović Z., Malgeri M., Ed. 2018, pp. 185–197.

[8] S. Sakhavi, C. Guan, and S. Yan, "Learning Temporal Information for Brain-Computer Interface Using Convolutional Neural Networks," *IEEE Trans. Neural Networks Learn. Syst.*, vol. 29, no. 11, pp. 5619–5629, 2018.

[9] L. F. Nicolas-Alonso and J. Gomez-Gil, "Brain computer interfaces, a review," *Sensors*, vol. 12, no. 2, pp. 1211–1279, 2012.

[10] L. Duan, Z. Hongxin, M. S. Khan, and M. Fang, "Recognition of motor imagery tasks for BCI using CSP and chaotic PSO twin SVM," *J. China Univ. Posts Telecommun.*, vol. 24, no. 3, pp. 83–90, 2017.

[11] M. Aljalal, R. Djemal, and S. Ibrahim, "Robot Navigation Using a Brain Computer Interface Based on Motor Imagery," *J. Med. Biol. Eng.*, vol. 39, no. 4, pp. 508–522, 2019.

[12] S. Sethi, R. Upadhyay, and H. S. Singh, "Stockwell-common spatial pattern technique for motor imagery-based Brain Computer Interface design," *Comput. Electr. Eng.*, vol. 71, no. July, pp. 492–504, 2018.

[13] M. Tangermann *et al.*, "Review of the BCI competition IV," *Front. Neurosci.*, vol. 6, no. 55, pp. 1–31, 2012.

[14] H. Cho, M. Ahn, S. Ahn, M. Kwon, and S. C. Jun, "EEG datasets for motor imagery brain-computer interface," *Gigascience*, vol. 6, no. 7, pp. 1–8, 2017.

[15] A. F. Perez-Zapata, A. F. Cardona-Escobar, J. A. Jaramillo-Garzon, and G. M. Dıaz, "Deep Convolutional Neural Networks and Power Spectral Density Features for Motor Imagery Classification of EEG Signals," *Augment. Cogn. Intell. Technol.*, vol. 10915, no. Schmorrow D., Fidopiastis C. (eds), pp. 158–169, 2018.

[16] L. Taylor and G. Nitschke, "Improving Deep Learning using Generic Data Augmentation," in *Proceedings of the IEEE Symposium Series on Computational Intelligence (SSCI)*, 2017, pp. 1542–1547.

[17] H. Cho, M. Ahn, and S. C. Jun, "A Step-by-Step Tutorial for a Motor Imagery–Based BCI," in *Brain–Computer Interfaces Handbook: Technological and Theoretical Advances*, no. March, Taylor & Francis Group, 2018, pp. 445–460.

[18] I. The MathWorks, "CWT," *Continuous 1-D wavelet transform*, 2016. [Online]. Available: https://www.mathworks.com/help/wavelet/ref/cwt.html. [Accessed: 12-Nov-2019].

[19] G. Pfurtscheller, C. Neuper, and J. Kalcher, "40-Hz oscillations during motor behavior in man," *Neurosci. Lett.*, vol. 164, no. 1–2, pp. 179–182, 1993.

[20] G. Pfurtscheller and F. H. Lopes da Silva, "Event-related EEG/MEG synchronization and desynchronization: basic principles," *Clin. Neurophysiol.*, vol. 110, no. 11, pp. 1842–1857, 1999.

[21] N. Lu, T. Li, X. Ren, and H. Miao, "A Deep Learning Scheme for Motor Imagery Classification based on Restricted Boltzmann Machines," *IEEE Trans. Neural Syst. Rehabil. Eng.*, vol. 25, no. 6, pp. 566–576, 2017.

[22] R. B. Braga, C. D. Lopes, and T. Becker, "Round Cosine Transform Based Feature Extraction of Motor Imagery EEG Signals," *World Congr. Med. Phys. Biomed. Eng.*, vol. 68, no. 2, pp. 511–515, 2019.

[23] Y. Zhang, C. S. Nam, G. Zhou, J. Jin, X. Wang, and A. Cichocki, "Temporally Constrained Sparse Group Spatial Patterns for Motor Imagery BCI," *IEEE Trans. Cybern.*, vol. 49, no. 9, pp. 3322–3332, 2018.

[24] A. Jiang, J. Shang, X. Liu, Y. Tang, H. K. Kwan, and Y. Zhu, "Efficient CSP Algorithm with Spatio-Temporal Filtering for Motor Imagery Classification," *IEEE Trans. Neural Syst. Rehabil. Eng.*, vol. 28, no. 4, pp. 1006–1016, 2020.